Diagn Interv Radiol 2020; 26:355–362

MUSCULOSKELETAL IMAGING

ORIGINAL ARTICLE

Is bone marrow edema syndrome a precursor of hip or knee osteonecrosis? Results of 49 patients and review of the literature

Tobias Geith
Ann-Cathrin Stellwag
Peter E. Müller
Maximilian Reiser
Andrea Baur-Melnyk

PURPOSE
Diagnosis of bone marrow edema syndrome (BMES) can be challenging. There is sometimes uncertainty about the correct diagnosis of BMES on morphologic magnetic resonance imaging (MRI), since subchondral findings like lines and spots can be misinterpreted as "beginning" or "possible" avascular osteonecrosis (AVN). The aim of our study was to systematically assess the temporal course of BMES from first diagnosis on MRI until the end of clinical symptoms and the full disappearance of bone marrow edema (BME) to determine whether subchondral lines and spots detected in these patients can develop into osteonecrosis.

METHODS
In a combined retrospective and prospective study, we retrieved serial MRI scans of hips and knees with BME from the hospital database. According to clinical and imaging data, all patients with degenerative, infectious/inflammatory, rheumatic, neoplastic conditions and those showing typical osteonecrosis were excluded. We collected all available MRI examinations from first detection of BME until its disappearance. In case edema had not fully resolved in the last available MRI scan, we performed an MRI with an additional dynamic contrast-enhanced (DCE-MRI) sequence. For each MRI scan, we recorded the severity of edema, the presence of subchondral hypointense lines and the presence of subchondral focal hypointense zones on T1-weighted images by two independent readers. The DCE-MRI scans were used to calculate parameter maps to assess the perfusion characteristics.

RESULTS
The study comprised 49 patients aged 22–71 years. In total, 171 morphologic and 5 DCE-MRI scans were evaluated. In 44 patients (89.8%), the BMES completely healed without remnants. In 18 of 49 patients (36.7%), a subchondral line was present in the first MRI exam. Nine patients (18.4%) developed a subchondral line within 1–5 months after the first MRI. In total, 27 out of 49 patients (55.1%) had subchondral lines (12 knees, 15 hips) during the timeframe of the study. All subchondral lines disappeared in the timeframe of the study. Subchondral focal hypointense zones were present in 14 out of 49 patients (28.6%): in 9 cases, subchondral focal hypointense zones disappeared after a median of 5.5 months (range, 1–85 months), while in 5 cases, subchondral focal lesions persisted until the end of the study (up to more than 85 months) without edema in the surrounding bone. All persisting subchondral focal lesions were hyperperfused. These 5 patients had associated meniscal lesions.

CONCLUSION
Our study shows that subchondral lines and spots found in patients with BMES do not develop into AVN. Subchondral lines, which resemble subchondral insufficiency fractures, are associated with BMES. Subchondral focal T1-hypointense zones do not represent AVN; most probably these areas represent reparative processes within the subchondral bone, where tensile and shear force overload is present due to altered biomechanics.

From the Department of Interventional Radiology (T.G. ✉ *tobias.geith@tum.de*), Rechts der Isar Hospital, Technical University of Munich, Munich, Germany; Departments of Radiology (A.C.S., M.R., A.B.M.), and Orthopedic Surgery (P.M.), University Hospital, Ludwig-Maximilians-University Munich, Munich, Germany.

Received 10 April 2019; revision requested 10 June 2019; last revision received 08 November 2019; accepted 24 November 2019.

Published online 15 June 2020.

DOI 10.5152/dir.2020.19188

The bone marrow edema syndrome (BMES) is a self-limiting disease whose etiology is not yet fully understood. Patients typically suffer from stress-related pain and impaired mobility. On MRI, the bone marrow edema (BME) manifests as an ill-defined area with hyperintense signal intensity on T2-weighted fat-saturated sequences and hypointense signal intensity on T1-weighted sequences (1). BMES mostly affects middle-aged patients. The migration of the BMES into another area of the same bone or into other joints

You may cite this article as: Geith T, Stellwag AC, Müller P, Reiser M, Baur-Melnyk A. Is bone marrow edema syndrome a precursor of hip or knee osteonecrosis? Results of 49 patients and review of the literature. Diagn Interv Radiol 2020; 26:355–362.

is possible (2–8). It is subject to controversial discussions as to whether subchondral insufficiency fractures or microfractures are the underlying reason for a BMES. Avascular necrosis (AVN) is an important differential diagnosis of BMES, since it also presents with pain and impaired mobility and affects mainly the subchondral bone. In AVN, impaired perfusion leads to osteocyte damage and necrosis, which often ends in an infraction of the subchondral bone (9). The ongoing controversy about the etiology and natural history of BMES and AVN highlights the importance of a correct diagnosis since this influences a proper and effective therapy. There is sometimes diagnostic uncertainty about the correct diagnosis of BMES on morphologic magnetic resonance imaging (MRI), since subchondral findings like lines and spots can be misinterpreted as "beginning" or "possible" AVN. Only a limited number of studies have examined the time course of BMES (10, 11). Many pieces of the puzzle must be collected in order to properly understand the disease and thus be able to treat it.

The aim of our study was to systematically assess the temporal course of BMES from first diagnosis on MRI until the end of clinical symptoms and the full disappearance of BME to determine if subchondral lines and spots detected in these patients can develop into osteonecrosis.

Methods

For this study, institutional review board approval was obtained (Project Nr. 187-10). Informed consent was obtained from all research subjects. The study collective was filtered from the picture archiving and communication system (PACS) of our hospital and from a radiologic private practice institute.

Patients

We used the keyword search for MRI reports of the hip or knee including "transient bone marrow edema syndrome", "TBMES", "bone marrow edema syndrome", "BMES", "bone marrow edema", "BME", and "transient osteoporosis". A total of 3691 hits were recorded, including examinations with the corresponding expressions in the clinical request, and not only in the assessment of the examinations. All these studies were screened for the presence of BME. Subsequently, we used clinical information, laboratory data, and imaging to determine whether typical BMES was present, namely in the form of an ill-defined area with hyperintense signal intensity on short tau inversion recovery (STIR) or proton density (PD)-weighted fat-saturated sequences and hypointense signal intensity on T1-weighted sequences. Inclusion criteria were an acute onset of pain in the joint, the absence of trauma, and the confirmation of spontaneous resolution of symptoms and BME only with conservative treatment, as shown in the follow-up data. Exclusion criteria were all other conditions leading to BME in the subchondral bone, namely patients with joint or bone infection, rheumatoid arthritis, osteoarthritis, trauma, tumor, and typical osteonecrosis. Imaging characteristics of these entities are well known and described in the literature (12–15). We put emphasis on the correct assessment of the shape of the low-intensity band on either T1-weighted or PD-weighted fat-saturated images, which in osteonecrosis has a smooth, concave appearance and circumscribes all the necrotic segments, while in subchondral insufficiency fractures it is generally irregular, serpiginous, and convex to the articular surface (16). Patients who had one of the exclusion criteria were not included. The evaluation of all examinations was performed by two radiologists experienced in musculoskeletal imaging for over 10 and 7 years. This ultimately resulted in 52 patients with BMES. The patients who still had a BME in the last performed MRI were contacted by phone. In total, 3 of the 52 patients could not be reached (1 patient died, 2 were no longer resident at the address / telephone number). Thus, the study group comprised 49 patients. We contacted the patients eligible for the study to inquire whether external MRI scans had been performed in the meantime, or whether they would be available for a follow-up MRI. In total, 171 MRI examinations and five dynamic contrast-enhanced MRI scans were examined in this study (49 baseline and 122 follow-up examinations).

Main points

- Subchondral lines and spots in patients with bone marrow edema syndrome do not develop into osteonecrosis.
- Subchondral insufficiency fractures are associated with bone marrow edema syndrome and may be the reason for the edema.
- Subchondral hypointense zones in bone marrow edema syndrome may represent reparative processes.

MRI examinations

MRI examinations were performed on scanners with magnetic field strengths of 1.5 and 3 Tesla (Skyra, Verio, Aera, Avanto and Symphony, Siemens Healthineers GmbH).

The sequence characteristics of the examinations in the radiologic private practice institute were as follows:

Sequences for hip examinations were a coronal proton density (PD)-weighted sequence with TR/TE, 3070/26 ms; bandwidth, 150 Hz/pixel; matrix, 358×512; field of view (FOV), 380×380 mm^2; flip angle, 180°; a coronal T1-weighted sequence with TR/TE, 647/15 ms; bandwidth, 120 Hz/pixel; matrix, 448×640; FOV, 380×380 mm^2; flip angle, 180°; an axial PD-weighted sequence with TR/TE, 4440/36 ms; bandwidth, 160 Hz/pixel; matrix, 202×512; FOV, 380×380 mm^2; flip angle, 180°; and a sagittal PD-weighted sequence with TR/TE, 3900/36 ms; bandwidth, 150 Hz/pixel; matrix, 244×384; FOV, 220×220 mm^2; flip angle, 176°.

Sequences for knee examinations were a coronal PD-weighted sequence with TR/TE, 2830/41 ms, bandwidth, 149 Hz/pixel, matrix 314×448, FOV 150×150 mm^2, flip angle, 180°; a coronal PD-weighted sequence with TR/TE, 2640/26 ms; bandwidth, 149 Hz/pixel; matrix, 247×448; FOV, 150×150 mm^2; flip angle, 180°; a coronal T1-weighted sequence with TR/TE, 500/12 ms; bandwidth, 140 Hz/pixel; matrix, 274×448; FOV, 150×150 mm^2; flip angle, 180°; and an axial PD-weighted sequence with TR/TE, 4000/38 ms; bandwidth, 151 Hz/pixel; matrix, 274×448; FOV, 150×150; flip angle, 180°.

The sequence characteristics of the examinations in our hospital were as follows:

Sequences for hip examinations were a coronal PD-weighted sequence with TR/TE, 3430/39 ms; bandwidth, 264 Hz/pixel; matrix, 356×512; FOV 380×380 mm^2; flip angle, 180°; a coronal T1-weighted sequence with TR/TE, 600/20 ms; bandwidth, 250 Hz/pixel; matrix, 346×512; FOV, 380×380 mm^2; flip angle, 150°; an axial PD-weighted sequence with TR/TE, 2700/26 ms; bandwidth, 130 Hz/pixel; matrix, 256×320; FOV, 160×160; flip angle, 148°; and a sagittal PD-weighted sequence with TR/TE, 3270/33 ms; bandwidth, 252 Hz/pixel; matrix, 256×320; FOV, 160×160 mm^2; flip angle, 140°.

Sequences for knee examinations were a coronal PD-weighted sequence with TR/TE, 3630/28 ms; bandwidth, 119 Hz/pixel; matrix, 304×320; FOV, 160×160; flip angle, 180°; a sagittal PD-weighted sequence with

TR/TE, 3890/27 ms; bandwidth, 119 Hz/pixel; matrix, 288×320; FOV, 170×170 mm^2; flip angle, 180°; an axial PD-weighted sequence with TR/TE, 4000/38 ms; bandwidth, 151 Hz/pixel; matrix, 274×448; FOV, 150×150 mm^2; flip angle, 90°; and a coronal T1-weighted sequence with TR/TE, 653/16 ms; bandwidth, 85 Hz/pixel; matrix, 365×384; FOV, 170×170 mm^2; flip angle, 90°.

Table 1. Grading of the BME

	0	1	2	3	4
Hip	No BME	BME <50% of femoral head	BME >50% of femoral head	BME including femoral neck	BME including intertrochanteric region
Knee	No BME	BME <50% of epiphysis	BME >50% of epiphysis	BME including metaphysis	BME including diaphysis

BME, bone marrow edema.

Evaluation of BME

We evaluated the baseline and follow-up examinations for the presence of BME and its extension within the bone marrow of the hip or the knee according to a visual scale which was adapted from Malizos et al. (11) as shown in Table 1. We regarded grade 0 as endpoint and fully healed BMES. If the last available MRI examination still revealed a BME, we assessed its extension, and the patient received a follow-up MRI. If this still showed BME, the patient received a further follow-up MRI after 6–8 weeks of reduced weight bearing.

We also recorded the presence of subchondral focal hypointense zones. This was defined as a subchondral zone, which appears round or biconvex in shape and shows strong hypointensity on T1-weighted images. This was first described by Vande Berg (17). We measured the size of the subchondral focal hypointense zone in its left-right and craniocaudal extent and calculated the area in cm^2.

In five patients with BMES of the knee, a subchondral focal hypointense zone remained in the follow-up for more than one year after the initial MRI scan. These patients received an additional MRI including a dynamic contrast-enhanced perfusion sequence with high temporal resolution to assess blood perfusion within these areas. The perfusion studies were performed with a fast three-dimensional gradient echo sequence with an effective temporal resolution of 3.3 s. Sixteen parallel coronal slices with 37.5% oversampling were measured to depict both the lesion in the joint and the popliteal artery. The lumen of the popliteal artery was used to determine the arterial input function. A slice thickness of 4 mm and a square FOV with 160×160 mm^2 was selected. The following parameters were used: TR/TE, 4.78/2.46 ms; matrix 256×245; 18° flip angle; bandwidth 500 Hz per pixel. Dynamic imaging was accelerated by partial k-space sampling and parallel imaging (GRAPPA technique, acceleration factor 3, 24 reference lines). Further improvement in temporal resolution was achieved using time-resolved angiography with stochastic trajectories (TWIST) with a central region of 17% and a peripheral scan density of 25%. To calculate the baseline, image data was taken over a period of 10 s prior to contrast administration. Subsequently, a bolus containing 0.1 mmol/kg of a 0.5 mol/L gadopentetate dimeglumine solution (Magnevist, Bayer Schering Pharma) was injected intravenously at 3 mL/s, followed by a 25 mL saline bolus. In total, 106 dynamic image stacks were acquired. The total measurement time for the dynamic contrast-enhanced sequence was 5 min and 54 s.

The evaluation of dynamic contrast-enhanced MRI was carried out with the software PMI 0.4, Platform for Research in Medical Imaging (18). The studies were assessed independently by two radiologists. For statistical analysis, divergent cases were reevaluated by the two radiologists who formed a consensus decision after careful consideration and discussion of the image features. We performed first an independent reading of the images and second a consensus reading where discrepancies were clarified. Consensus was reported by the two radiologists after reading and discussing all images and the results from the independent reading session, as if only one observer had read the images. Inter-rater reliability was calculated using Cohen's-kappa. Kappa values <0 indicated no agreement, 0–0.20 indicated slight, 0.21–0.40 fair, 0.41–0.60 moderate, 0.61–0.80 substantial, and 0.81–1 indicated almost perfect agreement. Kappa values for the independent reading and the results of the consensus reading are shown in the results section herein.

A model-free deconvolution analysis, which did not include assumptions on the internal structure of the tissue, was performed to produce parameter maps of plasma flow (PF) and mean transit time (MTT). A region-of-interest was defined in the lumen of the external iliac or the popliteal artery respectively to extract the arterial input function. Maps of PF were calculated on a pixel-by-pixel basis as the maximum of the impulse response function, and maps of MTT were calculated as the ratio of the time integral to the maximum impulse response function for each pixel (19, 20).

All MRI scans were read for the presence of subchondral insufficiency fractures (SIF) (21). SIF was diagnosed when a linear subchondral hypointense line was present on either T1-weighted or PD-weighted fat-saturated images within epiphyseal edema, which showed an irregular, serpiginous, and convex to the articular surface (16). The diameter was measured, and it was observed if they disappeared/healed over time.

Statistical analysis

The statistical evaluation of the results was done with MedCalc Statistical Software version 18 (MedCalc Software) using descriptive statistics. Descriptive statistics of the data are presented with n (%) and median (min-max) for non-normalized variables and as mean ± standard deviation (SD) for normal distributions. Normal distribution was tested with the Kolmogorov-Smirnov-Test, with $P < 0.05$ rejecting normal distribution. An alpha value of 0.05 was chosen.

Results

In this partially prospective and partially retrospective study, a total of 49 patients (21 women and 28 men) were included. An overview of the descriptive statistics is given in Table 2. The patient age was between 22 and 71 years with a mean age of 47.5±11.9 years (women 46.4±14 years, men 48.3±10.4 years) at the time of the first MRI scan. Twenty-one knee joints (42.9%, 9 female, 12 male) and 28 hip joints (57.1%, 12 female, 16 male) were evaluated.

The initial examination showed BME grade 1 in 2 patients (4.1%; 1 knee, 1 hip),

Table 2. Descriptive statistics of the patients with BME

	n (%)	mean±SD / median (range)
Age, all patients (years)	49 (100)	47.5±11.9
Women (years)	21 (42.9)	46.4±14
Men (years)	28 (57.1)	48.29±10.4
BME disappeared after (months)	44 (89.8)	9 (2–91)
Subchondral focal hypointense zone	14 (28.6)	
Horizontal extension (cm)		1.10±0.51
Craniocaudal extension (cm)		0.30 (0.1–0.90)
Area (cm^2)		0.47±0.39
Subchondral focal hypointense zone healed after (months)	9 (18.4)	5.5 (1–85)
SIF, n (%)	27 (55.1)	
Length (cm)		1.27±0.67
Occurrence after first MRI (months)		0.0 (0.0–5.0)
Healed after (months)		12.0 (1.0–69.0)

Data are presented as mean±SD (if the assumption of normality is provided) or median and min-max (if not normally distributed).
SD, standard deviation; BME, bone marrow edema; SIF, subchondral insufficiency fracture; MRI, magnetic resonance imaging.

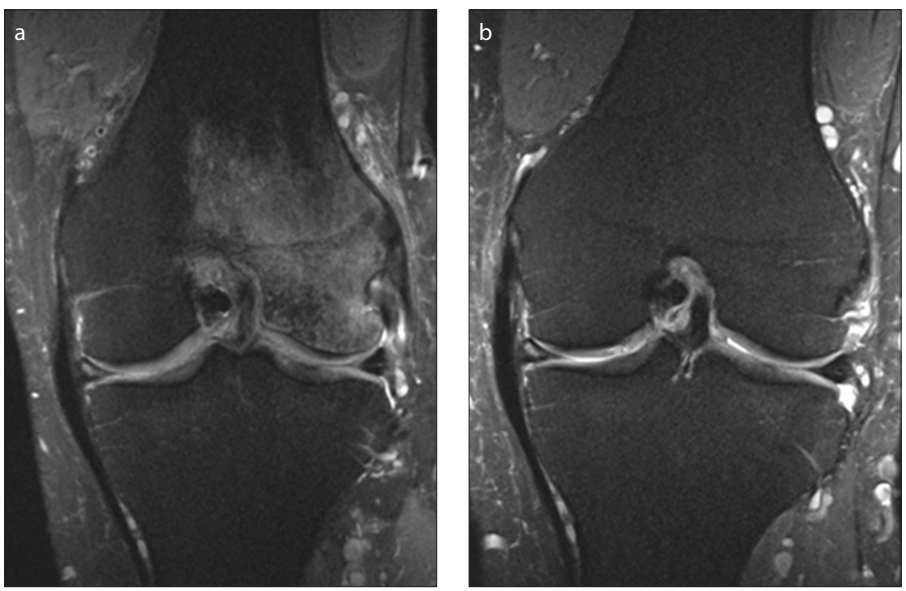

Figure 1. a, b. A 61-year-old patient with typical BMES and pain in his left knee joint, starting 2 months before baseline MRI after hiking. No trauma was reported. Coronal PD-weighted fat-saturated image **(a)** shows bone marrow edema (grade 4). Image **(b)** shows fully resolved bone marrow edema after 12 months.

grade 2 in 5 patients (10.2%; 5 knees), grade 3 in 20 patients (40.8%; 12 knees, 8 hips) grade 4 in 22 patients (44.9%; 3 knees, 19 hips). In 44 out of 49 patients (89.8%), MRI follow-up documented full disappearance of BMES after a median 9 months (range, 2–91 months) without any residual alterations (Fig. 1). For all examinations (baseline and follow-up) there was also almost perfect agreement between the two readers for assessing the presence and grade of BME (kappa values, 0.95–1.00).

In 14 out of 49 patients (28.6%), a subchondral focal hypointense zone was found (6 knees, 8 hips). At baseline, seven patients (50% of patients with subchondral focal hypointense zone) already showed a subchondral focal hypointense zone. The other seven patients (50% of patients with subchondral focal hypointense zone) showed a subchondral focal hypointense zone at one of the follow-up MRI scans after 1–4 months. Its mean horizontal extension was 1.10±0.51 cm and its median craniocaudal extension was 0.3 cm (range, 0.1–0.9 cm). The mean area of the subchondral focal hypointense zone was 0.47±0.39 cm^2. Nine subchondral focal hypointense zones (64.3% of patients with subchondral focal hypointense zone; i.e., 18.4% of all 49 patients) healed after a median of 5.5 months (range, 1–85 months). In five patients (35.7% of patients with subchondral focal hypointense zone; i.e., 10.2% of all 49 patients), the subchondral focal hypointense zone remained until the end of the study (more than 85 months after the initial MRI). This was only observed in knee joints and not in hips. The dynamic contrast-enhanced MRI with high temporal resolution showed strongly increased PF in the subchondral focal hypointense zones in all cases. All patients with these persistent lesions had damage in the adjacent meniscus without history of acute trauma (horizontal meniscal tear, n=3, 60% of patients with persistent lesions; meniscal protrusion, n=2, 40% of patients with persistent lesions) (Fig. 2). The agreement between the two readers was almost perfect in all examinations (baseline and follow-up) in the assessment of the subchondral focal zones (kappa values, 0.86–1.00).

In 27 out of 49 patients (55.1%), a SIF was detected (12 knees, 15 hips). In 18 patients (66.7% of patients with SIF; i.e., 55.1% of all 49 patients), a SIF was detected in the first MRI exam. The other 9 subjects (33.3% of patients with SIF; i.e., 18.4% of all 49 patients) developed a SIF within 1–5 months after the first MRI. The mean length of the SIFs was 1.27±0.67 cm. SIFs occurred after a median of 0.0 months (range, 0.0–5.0 months). All SIFs completely healed after a median of 12 months (range, 1–69 months) during the study (Fig. 3). The agreement between the two readers was almost perfect in all examinations (baseline and follow-up) in the assessment of SIF (kappa values, 0.98–1.00).

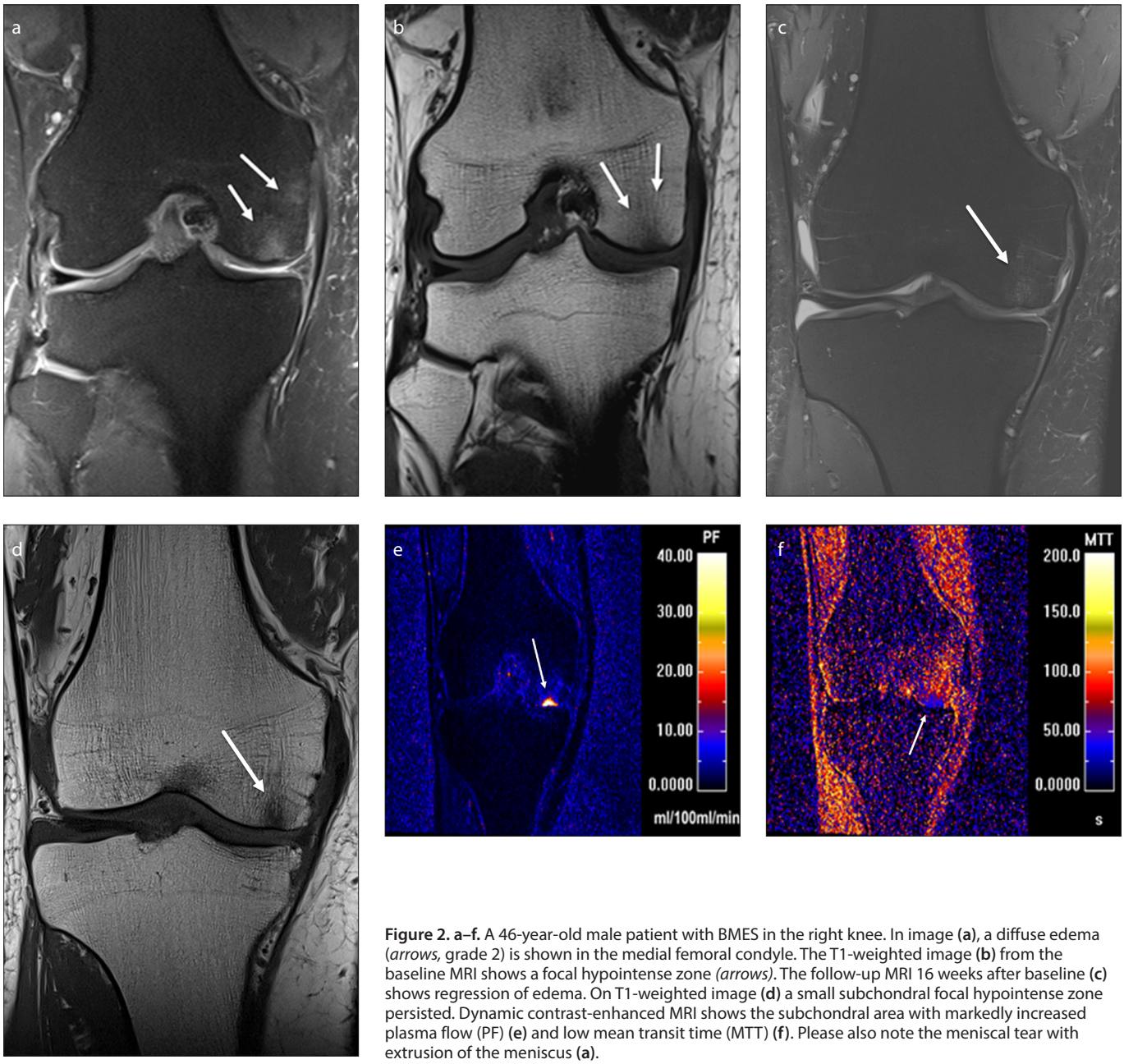

Figure 2. a–f. A 46-year-old male patient with BMES in the right knee. In image **(a)**, a diffuse edema (*arrows,* grade 2) is shown in the medial femoral condyle. The T1-weighted image **(b)** from the baseline MRI shows a focal hypointense zone *(arrows)*. The follow-up MRI 16 weeks after baseline **(c)** shows regression of edema. On T1-weighted image **(d)** a small subchondral focal hypointense zone persisted. Dynamic contrast-enhanced MRI shows the subchondral area with markedly increased plasma flow (PF) **(e)** and low mean transit time (MTT) **(f)**. Please also note the meniscal tear with extrusion of the meniscus **(a)**.

Discussion

The potential role of BME as a precursor of AVN has previously been debated controversially. Initially BME was considered as the early stage of AVN (22, 23). Three studies did not find BME in early stages of AVN before the appearance of the "band-like sign". Kim et al. (24) reviewed the MRI examinations of 200 patients with histologically confirmed AVN of the femoral head and found that BME was not seen before the band-like sign could be detected. BME was detected in two patients at stage II and in 53 patients at stage III AVN. Fujioka et al. (25) prospectively examined the hip MRI scans of 57 renal transplant recipients who received immunosuppression with steroids and cyclosporine A or FK506. The scans were performed preoperatively and after 3–6 weeks, 9–12 weeks, 24 weeks, and after 12 months. Twelve patients developed band like patterns typical for osteonecrosis. None of the 57 patients showed BME preceding osteonecrosis. Kubo et al. (26) examined 51 renal allograft recipients. At baseline, no patient showed abnormalities in MRI of the hips. In their study, 23 femoral heads showed a band-like pattern between 6 weeks and 12 months after transplantation. As in the other two studies, BME was not present prior to the appearance of the band-like signal changes. Meier et al. (27) showed that BME is a phenomenon which occurs in the advanced course of femoral head AVN. It represents failure of the spongy microarchitecture of the femoral head with the appearance of microfractures.

In our cohort of patients with BMES, we tested the contrary assumption, namely that BME never precedes osteonecrosis in the hip and knee. In 44 of the 49 patients, we found complete healing of the BME without any remnants. None of the 49 patients showed a "band-like sign" typical for osteonecrosis in any MRI.

Figure 3. a, b. A 44-year-old male patient with BMES in his left hip joint, starting 3 months before baseline MRI. No trauma was reported. PD-weighted fat-saturated image **(a)** shows extensive BME with a linear hypointense line corresponding to an insufficiency fracture in the left femoral head *(arrow)*. Both BME as well as the SIF are no longer present after 15 months **(b)**.

This is consistent with the studies of other authors. Karantanas et al. (28) retrospectively reviewed the MRI examinations of 22 patients with BMES of the knee. The patients had persistent knee pain for 2 weeks to 6 months before the first MRI scan. In addition, they were followed clinically for at least 2 years after complete resolution of symptoms and MRI findings. The BME healed in all patients without residual alterations. Malizos et al. (11) retrospectively reviewed the MRI examinations of 42 patients with hip-associated BMES. The first MRI scans were performed at a mean of 12.5 weeks after symptom onset and the second MRI scans at a mean of 24 weeks after symptom onset. Under conservative treatment with analgesics and antiresorptive medication combined with restriction of physical activities, all BMES healed within 18 months. Vande Berg (29) examined 67 patients with BMES in 72 affected hips. Apart from extension of edema, 3 subchondral lesions (SIF, focal subchondral hypointense zones, epiphyseal focal infraction) were identified. The majority of BME were transient and healed (57/72). In their study, 15 lesions especially larger subchondral hypointense zones (> 4 mm width and >12.5 mm in length) did not heal. Patients with lack of additional subchondral changes had a 100% positive predictive value to be transient.

Finally, in the study by Lecouvet et al. (30), which examined 23 nontraumatic lesions in 23 patients with bone marrow edema pattern in the femoral condyles, 14 lesions showed complete resolution and 9 lesions evolved to collapsed osteonecrosis. The authors concluded that absence of T2-hypointense subchondral areas on the initial T2-weighted images was always indicative of complete reversibility at follow-up, whereas lesions that showed such low-signal intensity subchondral areas could be either transient or irreversible. Notably, they found that a cutoff length of more than 14 mm or a thickness of more than 4 mm were indicative of evolution to collapsed osteonecrosis. However, the authors noted that the exact significance of these subchondral areas remained unknown (30). In our study, we observed subchondral hypointense areas smaller than the cutoff dimensions defined by Lecouvet et al. (30), namely, with a mean horizontal extension (i.e., length) of 1.10± 0.51 cm and a median craniocaudal extension (i.e., thickness) of 0.30 cm (0.10–0.90 cm). Such hypointense areas did not evolve to collapsed osteonecrosis.

In our cohort, we detected subchondral focal hypointense zones in 14 of 49 patients, which were no longer detectable in 9 patients after a median of 5.5 months (1.0–85.0 months). They showed round or oval shaped strong hypointensity on T1-weighted images and slightly increased signal intensity on PD-weighted fat-saturated images (Fig. 2). We were able to show that these subchondral focal hypointense zones present with a markedly elevated PF, which corresponds to a high perfusion of the bone marrow in this area thereby excluding AVN. The perfusion pattern of these subchondral remnants has not been described before. It was often assumed that these lesions represent focal necrotic zones, which is proved wrong by our results. Our findings contribute to elucidating the significance of small subchondral hypointense areas (i.e., having a length of 14 mm or less or a thickness of 4 mm or less) by showing that these are either transient or persistent but with high perfusion. These observations can likely be attributed to the presence of reparative tissue.

The discrimination of AVN and BMES with perfusion imaging was assessed in two former studies. Mueller et al. (31) examined 29 patients with painful hip and BME pattern of the proximal femur with diffusion-weighted and dynamic contrast-enhanced sequences. They used a T1-weighted fast low-angle shot sequence with a temporal resolution of 10 s per image stack. Maximum enhancement in the epiphysis was significantly higher in patients with SIFs and patients with BMES compared with patients with AVN. SIF and BMES showed no significantly different perfusion pattern. The authors explain the hyperemia of the epiphysis in SIF patients with reparative changes and a fracture related hyperperfusion (31). Geith et al. (32) also found a hyperperfusion in the subchondral epiphyseal bone in patients with BMES. They examined 19 joints with BMES and 17 joints with AVN using dynamic perfusion MRI with high temporal resolution, and calculated parameter maps for PF and MTT. The study revealed two perfusion patterns, which did not overlap: BMES showed a subchondral focal to linear area of high PF. Osteonecrosis, on the other hand, revealed a convex focal subchondral area with low or no detectable PF adjacent to the joint surface, which was surrounded by a rim of high PF consistent with the hyperperfused granulation wall in AVN (32).

In the present study, all 5 patients with persisting subchondral focal hypointense zones were located at the knee and had a degenerative meniscal tear or meniscal extrusion without a history of acute trauma or osteoarthritis. Other studies showed that meniscal damage can lead to a BMES in the affected compartment of the knee joint and that patients with meniscal damage are at a higher risk. The extent depended on the severity of the meniscal damage. Some authors attribute BME in these patients to disturbed biomechanics (33, 34). We also regard this mechanical damage as a possible cause of disturbed transmission of the pressure force between the articular surfaces in the knee joint. This is likely to result in persistent over-loading that prevents microfractures from healing.

SIF can be detected most sensitively using MRI (35). They were described by Vande Berg et al. (29) in 1996 in a series of renal transplant recipients. SIF appear as a linear hypointense signal paralleling the articular surface on T1-weighted or PD-weighted fat-saturated sequences associated with BME (Fig. 3). Insufficiency fractures are caused by a weakening of the bone in osteopenia or osteoporosis combined with normal loading or minor trauma. Predominantly, older and postmenopausal women are affected. Meniscal damage and meniscal resections are a risk factor for developing SIF in the knee. Originally, these lesions were termed spontaneous osteonecrosis of the knee, but recent studies define them as insufficiency fractures (36, 37). In our study, 55.1% of the patients showed SIF during the study period. In 18 patients, a SIF was detected in the first MRI. The other 9 subjects showed a SIF within one to five months after the first MRI. All SIF healed over time.

Malizos et al. (11) found a prevalence of insufficiency fractures of about 4% in 42 patients with BMES of the hip, which all healed over time. Klontzas et al. (38) retrospectively evaluated 155 hips for the presence of SIF. In 48.7% of their study group, subchondral changes corresponding to SIF were detected. All patients in their study recovered completely with conservative treatment. No cases progressed to AVN. DEXA scans in this study showed that all patients had decreased osteodensity (either osteopenia or osteoporosis). This supports the hypothesis that insufficiency fractures may be the cause of weakened bone or overload and lead secondarily to BME. Another risk factor for developing SIF are cartilage defects. Hackney et al. (39) retrospectively evaluated the MRI examinations of 51 patients with SIF at the knee and found a significant association of SIF and cartilage defect size. Patients with cartilage defects or osteoarthritis were not included in our series.

Vande Berg et al. (17) prospectively examined 67 patients with BMES of the femoral head. The patients had equivocal radiographic findings. Follow-up took place after at least 24 months up to 72 months to determine the outcome of the lesions. Of 72 lesions, 57 proved to be transient and healed within 12–72 months. During their study, 44% of the patients showed subchondral hypointense lines, consistent with SIFs, similar in frequency to our study. The frequency of SIF was not significantly different between irreversible and transient lesions. In contrast to the study of Vande Berg (17), all patients with SIF in our study group healed completely with reduced weight bearing.

We hypothesize that in most of the cases with BMES without any other articular structural changes, SIF triggers the BMES. SIF can be detected in the early course of the disease; they always occur at the lower extremity where weight bearing plays a major role, and they are associated with osteoporosis. According to our results and the literature cited above, SIF and BME will resolve when conservative therapy with weight bearing reduction is employed. Severe edema may mask a SIF so that it may not be detectable in every case at first MRI. This may be the reason why some SIFs could not be detected in the baseline MRI study in our cohort or why some authors report a lower rate of SIF in BMES.

A possible limitation of our study is that histologic correlation was not available due to ethical reasons, since treatment of BMES does not include surgical treatments with the possibility to acquire bone samples. Another limitation is that the patients did not receive follow-up MRI examinations in definite periods of time, so that the time course between the MRI exams differed in parts strongly. However, all patients who were enrolled, received follow-up MRIs until the complete resolution of symptoms and MRI alterations.

In conclusion, our study shows that subchondral lines and spots, which can be found in patients with BMES, do not develop into AVN. Subchondral insufficiency fractures are associated with BMES and are probably the reason for TBMES of the hip and knee since they occur in early course of the disease and resolve after reduction of weight bearing. Subchondral focal T1-hypointense zones do not represent AVN; most probably, these areas represent reparative processes within the subchondral bone where tensile and shear force overload is present due to altered biomechanics.

Conflict of interest disclosure

The authors declared no conflicts of interest.

References

1. Wilson AJ, Murphy WA, Hardy DC, Totty WG. Transient osteoporosis: transient bone marrow edema? Radiology 1988; 167:757–760. [Crossref]
2. Hofmann S, Kramer J, Vakil-Adli A, Aigner N, Breitenseher M. Painful bone marrow edema of the knee: differential diagnosis and therapeutic concepts. Orthop Clin North Am 2004; 35:321–333. [Crossref]
3. Guerra JJ, Steinberg ME. Distinguishing transient osteoporosis from avascular necrosis of the hip. J Bone Joint Surg Am Vol 1995; 77:616–624. [Crossref]
4. Doury P. Bone-marrow oedema, transient osteoporosis, and algodystrophy. J Bone Joint Surg Br 1994; 76:993–994. [Crossref]
5. Bartl C, Imhoff A, Bartl R. Treatment of bone marrow edema syndrome with intravenous ibandronate. Arch Orthop Trauma Surg 2012; 132:1781–1788. [Crossref]
6. Blum A. Bone Marrow Edema Sydrome. In: Baur-Melnyk A, editor. Magnetic Resonance Imaging of the Bone Marrow. Berlin Heidelberg: Springer; 2012, 247–263. [Crossref]
7. Patel S. Primary bone marrow oedema syndromes. Rheumatology 2014; 53:785–792. [Crossref]
8. Karantanas AH, Drakonaki E, Karachalios T, Korompilias AV, Malizos K. Acute non-traumatic marrow edema syndrome in the knee: MRI findings at presentation, correlation with spinal DEXA and outcome. Eur J Radiol 2008; 67:22–33. [Crossref]
9. Saini A, Saifuddin A. MRI of osteonecrosis. Clinical Radiol 2004; 59:1079–1093. [Crossref]
10. Klontzas ME, Vassalou EE, Zibis AH, Bintoudi AS, Karantanas AH. MR imaging of transient osteoporosis of the hip: An update on 155 hip joints. Eur J Radiol 2015; 84:431–436. [Crossref]
11. Malizos KN, Zibis AH, Dailiana Z, Hantes M, Karachalios T, Karantanas AH. MR imaging findings in transient osteoporosis of the hip. Eur J Radiol 2004; 50:238–244. [Crossref]
12. Fotiadou A, Karantanas A. Osteonecrosis and Bone Infarction. In: Baur-Melnyk A, editor. Magnetic Resonance Imaging of the Bone Marrow. Berlin, Heidelberg: Springer Berlin Heidelberg; 2012, 221–246. [Crossref]
13. Narvaez JA, Narváez J, De Lama E, De Albert M. MR Imaging of early rheumatoid arthritis. Radiographics 2010; 30:143–163. [Crossref]
14. Menashe L, Hirko K, Losina E, et al. The diagnostic performance of MRI in osteoarthritis: a systematic review and meta-analysis. Osteoarthritis Cartilage 2012; 20:13–21. [Crossref]
15. Nascimento D, Suchard G, Hatem M, de Abreu A. The role of magnetic resonance imaging in the evaluation of bone tumours and tumour-like lesions. Insights Imaging 2014; 5:419–440. [Crossref]
16. Ikemura S, Yamamoto T, Motomura G, Nakashima Y, Mawatari T, Iwamoto Y. MRI evaluation of collapsed femoral heads in patients 60 years old or older: Differentiation of subchondral insufficiency fracture from osteonecrosis of the femoral head. AJR Am J Roentgenol 2010; 195:W63–68. [Crossref]
17. Vande Berg BC, Malghem JJ, Lecouvet FE, Jamart J, Maldague BE. Idiopathic bone marrow edema lesions of the femoral head: predictive value of MR imaging findings. Radiology 1999; 212:527–535. [Crossref]
18. Sourbron S, Biffar A, Ingrisch M. PMI: platform for research in medical imaging. ESMRMB09; Antalya. Vienna, Austria: European Society for Magnetic Resonance in Medicine and Biology; 2009.
19. Sourbron S, Dujardin M, Makkat S, Luypaert R. Pixel-by-pixel deconvolution of bolus-tracking data: optimization and implementation. Phys Med Biol 2007; 52:429–447. [Crossref]

20. Biffar A, Schmidt GP, Sourbron S, et al. Quantitative analysis of vertebral bone marrow perfusion using dynamic contrast-enhanced MRI: initial results in osteoporotic patients with acute vertebral fracture. J Magn Reson Imaging 2011; 33:676–683. [Crossref]
21. Yamamoto T. Subchondral insufficiency fractures of the femoral head. Clin Orthop Surg 2012; 4:173–180. [Crossref]
22. Mitchell DG, Rao VM, Dalinka MK, et al. Femoral head avascular necrosis: correlation of MR imaging, radiographic staging, radionuclide imaging, and clinical findings. Radiology 1987; 162:709–715. [Crossref]
23. Turner DA, Templeton AC, Selzer PM, Rosenberg AG, Petasnick JP. Femoral capital osteonecrosis: MR finding of diffuse marrow abnormalities without focal lesions. Radiology 1989; 171:135–140. [Crossref]
24. Kim YM, Oh HC, Kim HJ. The pattern of bone marrow oedema on MRI in osteonecrosis of the femoral head. J Bone Joint Surg Br 2000; 82:837–841. [Crossref]
25. Fujioka M, Kubo T, Nakamura F, et al. Initial changes of non-traumatic osteonecrosis of femoral head in fat suppression images: bone marrow edema was not found before the appearance of band patterns. Magn Reson Imaging 2001; 19:985–991. [Crossref]
26. Kubo T, Yamazoe S, Sugano N, et al. Initial MRI findings of non-traumatic osteonecrosis of the femoral head in renal allograft recipients. Magn Reson Imaging 1997; 15:1017–1023. [Crossref]
27. Meier R, Kraus TM, Schaeffeler C, et al. Bone marrow oedema on MR imaging indicates ARCO stage 3 disease in patients with AVN of the femoral head. Eur Radiol 2014; 24:2271–2278. [Crossref]
28. Karantanas AH, Nikolakopoulos I, Korompilias AV, Apostolaki E, Skoulikaris N, Eracleous E. Regional migratory osteoporosis in the knee: MRI findings in 22 patients and review of the literature. Eur J Radiol 2008; 67:34–41. [Crossref]
29. Vande Berg BC, Malghem J, Goffin EJ, Duprez TP, Maldague BE. Transient epiphyseal lesions in renal transplant recipients: presumed insufficiency stress fractures. Radiology 1994; 191:403–407. [Crossref]
30. Lecouvet FE, van de Berg BC, Maldague BE, et al. Early irreversible osteonecrosis versus transient lesions of the femoral condyles: prognostic value of subchondral bone and marrow changes on MR imaging. AJR Am J Roentgenol 1998; 170:71–77. [Crossref]
31. Mueller D, Schaeffeler C, Baum T, et al. Magnetic resonance perfusion and diffusion imaging characteristics of transient bone marrow edema, avascular necrosis and subchondral insufficiency fractures of the proximal femur. Eur J Radiol 2014; 83:1862–1869. [Crossref]
32. Geith T, Niethammer T, Milz S, Dietrich O, Reiser M, Baur-Melnyk A. Transient bone marrow edema syndrome versus osteonecrosis: perfusion patterns at dynamic contrast-enhanced MR imaging with high temporal resolution can allow differentiation. Radiology 2017; 283:478–485. [Crossref]
33. Lo GH, Hunter DJ, Nevitt M, Lynch J, McAlindon TE, Group OAII. Strong association of MRI meniscal derangement and bone marrow lesions in knee osteoarthritis: data from the osteoarthritis initiative. Osteoarthritis Cartilage 2009; 17:743–747. [Crossref]
34. Englund M, Guermazi A, Roemer FW, et al. Meniscal pathology on MRI increases the risk for both incident and enlarging subchondral bone marrow lesions of the knee: the MOST Study. Ann Rheum Dis 2010; 69:1796–1802. [Crossref]
35. Krestan C, Hojreh A. Imaging of insufficiency fractures. Eur J Radiol 2009; 71:398–405. [Crossref]
36. Ramnath RR, Kattapuram SV. MR appearance of SONK-like subchondral abnormalities in the adult knee: SONK redefined. Skeletal Radiol 2004; 33:575–581. [Crossref]
37. Yamamoto T, Bullough PG. Spontaneous osteonecrosis of the knee: the result of subchondral insufficiency fracture. J Bone Joint Surg Am 2000; 82:858–866. [Crossref]
38. Klontzas ME, Vassalou EE, Zibis AH, Bintoudi AS, Karantanas AH. MR imaging of transient osteoporosis of the hip: an update on 155 hip joints. Eur J Radiol 2015; 84:431–436. [Crossref]
39. Hackney LA, Lee MH, Joseph GB, Vail TP, Link TM. Subchondral insufficiency fractures of the femoral head: associated imaging findings and predictors of clinical progression. Eur Radiol 2016; 26:1929–1941. [Crossref]